Jurášek, L., and Smillie, L. B. (1973), *Can. J. Biochem. 51,* 1077.
Jurášek, L., and Smillie, L. B. (1974), *Can. J. Biochem. 52,* 382.
Krieger, M., Kay, L. M., and Stroud, R. M. (1974), *J. Mol. Biol. 83,* 209.
Landon, M. (1964), Ph.D. Thesis, University of Birmingham, England.
Offord, R. E. (1966), *Nature (London) 211,* 591.
Olafson, R. W. (1973), Ph.D. Thesis, University of Alberta, Edmonton, Alberta, Canada.
Olafson, R. W., and Smillie, L. B. (1975), *Biochemistry,* preceding paper.
Pisano, J. J., and Bronzert, T. J. (1969), *J. Biol. Chem. 224,* 5597.
Raftery, M. A., and Cole, R. D. (1966), *J. Biol. Chem. 241,* 3457.
Stroud, R. M., Kay, L. M., and Dickerson, R. E. (1971), *Cold Spring Harbor Symp. Quant. Biol. 36,* 125.
Stroud, R. M., Kay, L. M., and Dickerson, R. E. (1974), *J. Mol. Biol. 83,* 185.
Smithies, O., Gibson, D. Fanning, E. M., Goodfliesh, R. M., Gilman, J. G., and Ballantyne, D. L. (1971), *Biochemistry 10,* 4912.
Walsh, K. A., and Neurath, H. (1964), *Proc. Nat. Acad. Sci. U.S. 52,* 884.
Welinder, K. G., and Smillie, L. B. (1972), *Can. J. Biochem. 50,* 63.
Yamada, S., and Itano, H. A. (1966), *Biochim. Biophys. Acta 130,* 538.

Nuclear Magnetic Resonance Studies of Histone IV Solution Conformation†

A. Eugene Pekary,‡ Hsueh-Jei Li,§ Sunney I. Chan,* Chen-Jung Hsu, and Thomas E. Wagner#

ABSTRACT: The 220-MHz high-resolution proton magnetic resonance (PMR) spectrum of histone IV has been examined as a function of histone concentration, salt concentration, and pD. The hydrophobic C-terminal portion of the histone IV monomer appears to be largely PMR "invisible" indicating that this region of the polypeptide contains rigid secondary structure. Further loss of PMR resonance areas with increased histone IV concentration in neat D_2O has been attributed to self-aggregation involving a monomer–dimer equilibrium. An equilibrium between the monomer and large aggregates, on the other hand, appears to dominate at NaCl concentrations above 0.01 *M*. pD studies reveal an abrupt increase in histone IV aggregation at pD <0.8 and precipitation of histone IV at pD values in the neighborhood of its isoelectric point, pD $\simeq$ 11.

Cationic histones participate in nuclear chromatin function by forming electrostatic–hydrophobic complexes with anionic DNA (Lewin, 1969; 1970; Tanford, 1961; Bradbury et al., 1967; Smart and Bonner, 1971). In the presence of high ionic strength, however, such complex formation is suppressed (Hoare and Johns, 1971), presumably by counterion stabilization of the components. A similar complex destabilizing effect occurs when the pH lies outside the interval between the component isoelectric points. Nucleohistones may dissociate in this latter case because the sign of the component net charges will then be the same. For these reasons salt and acid extraction are the most commonly employed techniques for dissociating histones from purified nuclear chromatin (Elgin et al., 1971).

Upon dissociation from DNA, however, the polybasic histones experience increased aggregation, particularly at high ionic strengths (Tanford, 1961; Bradbury et al., 1967). Among the well-characterized histones, histone IV self-associates in electrolyte-containing media to the greatest extent (Diggle and Peacocke, 1971; Edwards and Shooter, 1969; Jirgensons et al., 1966). Investigations by optical rotatory dispersion (ORD) (Bradbury et al., 1965; Jirgensons and Hnilica, 1965; Tuan and Bonner, 1969), circular dichroism (CD) (Wagner, 1970; Shih and Fasman, 1971; Li et al., 1971), and CD and fluorescence (Li et al., 1972) have revealed that ionic strength changes affect not only the histone IV self-association tendency but also its conformation. According to these studies, the histone IV "extended coil" may acquire up to 20% α-helical content in uni-univalent salt solutions exceeding 0.1 *M*. Additional secondary and tertiary structure may also be present in the solution conformation of this histone since previous interpretations of ORD and CD spectra for "unordered" proteins based on a combination of random and helical segments may not have been entirely adequate (Dearborn and Wetlaufer, 1970; Li et al., 1971). The time course of changes in the his-

† From the Arthur Amos Noyes Laboratory of Chemical Physics, California Institute of Technology, Pasadena, California 91125 (Contribution No. 4565), and Cornell University Graduate School of Medical Sciences, New York, New York 10021. *Received July 18, 1974.* This work was supported by U.S. Public Health Service Grant GM-14523 from the National Institute of General Medical Sciences (to S.I.C.) and Grant CA-08748 from the National Cancer Institute (to T.E.W.).

‡ Population Council Postdoctoral Fellow, 1970–1972. Present address: Endocrinology Laboratory, Wadsworth VA Hospital, Wilshire and Sawtelle Boulevards, Los Angeles, California 90073.
§ Present address: Department of Chemistry, Brooklyn College of the City University of New York, Brooklyn, New York 11210.
# Present address: Department of Chemistry, Ohio University, Athens, Ohio 45701.

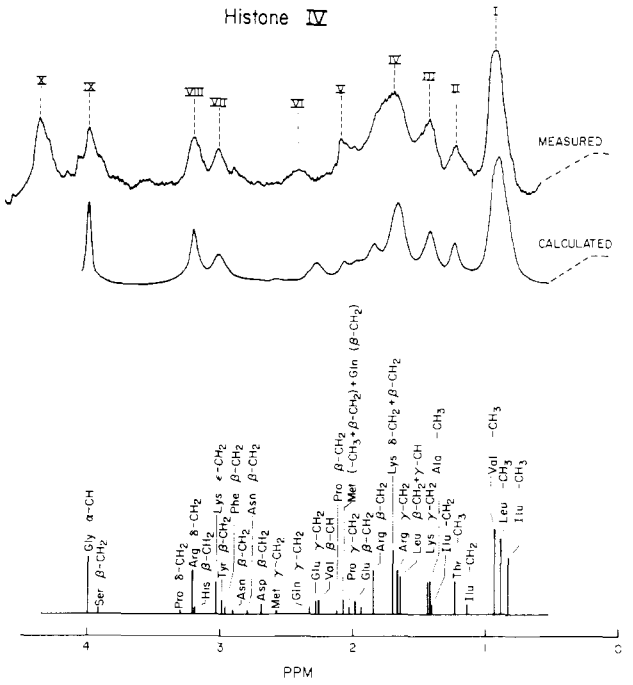

FIGURE 1: Observed and simulated 220-MHz PMR spectrum of histone IV in the high-field region. Histone concentration $[H_0] = 1.0 \times 10^{-3}$.

tone IV CD spectrum and fluorescence depolarization has also been examined after increasing the solution ionic strength (Li et al., 1972). The results suggest that histone IV undergoes a conversion from a significantly α-helical to a predominantly β-sheet conformation at a rate which increases with ionic strength.

Early proton magnetic resonance (PMR) studies on histone IV at 60 MHz (Bradbury et al., 1967) revealed some conspicuous alterations in the histone IV PMR spectrum with changes in the solvent or ionic strength. These PMR spectral changes were ascribed to variation in the α-helix content, and hence the segmental flexibility of those regions of histone IV which permit α-helix formation. More recent PMR investigations of histone IV at 100 MHz (Boublik et al., 1970) and 220 MHz (Bradbury and Rattle, 1972) were interpreted in terms of its amino acid sequence (DeLange et al., 1969; Ogawa et al., 1969). Relative area losses were observed for the PMR bands of the hydrophobic residues with increasing ionic strength. These modifications in PMR area were ascribed to a combination of secondary structure changes and histone–histone interactions.

This paper is the first of a series dealing with a more complete investigation of the conformational and aggregation properties of histone IV in aqueous solution using 220-MHz PMR spectroscopy. The present studies differ from the earlier PMR work of Boublik et al. (1970) and Bradbury and Rattle (1972) in at least one important respect. In addition to studies of the histone IV as a function of salt concentration, ionic strength, and pH, we have undertaken a systematic concentration study as well. We contend that such a concentration study is necessary if effects due to histone–histone interactions are to be sorted out from those arising from changes in the secondary structure of the polypeptide. This present report is concerned primarily with the interpretation of spectral results obtained in the high-field region of the PMR spectrum. Subsequent papers will include data obtained for histone IV in the low-field region as well as studies of histone IV fragments.

Materials and Methods

The histone 2a fraction was isolated from calf thymus tissue by the selective solvent extraction method (procedure 2) of Johns (1964). Histone IV was prepared from this fraction by a modification of the Sephadex gel filtration procedure of Starbuch et al. (1968). Histone thus prepared appears as a single band on polyacrylamide gel electrophoresis. The amino acid composition is completely consistent with that calculated from its sequence (DeLange et al., 1969; Ogawa et al., 1969).

Histone IV chloride was dissolved in 99.7% D_2O supplied by Columbia Organic Chemical Co., Inc. High-field region PMR spectra were obtained with a Varian HR-220 PMR spectrometer equipped with a Varian C-1024 time-averaging computer. A capillary containing 2,2-diphenyl-1-picrylhydrazyl (DPPH),[1] tetramethylsilane (Me_4Si), and $DCCl_3$ served as an area reference as well as a chemical shift reference for the histone IV spectra, since 1,1-dimethyl-2-silapentane-5-sulfonate (DSS), the reference compound usually used as an internal standard in such studies, was found to precipitate histone IV. The chemical shift of the DPPH-broadened Me_4Si external reference was measured relative to internal DSS in a separate experiment. This frequency difference was then used to refer all chemical shifts reported in this work to "internal" DSS.

Because of the uncertain base line, there is around 10–20% error in the area evaluations. The error will be larger for small, poorly resolved peaks. All area measurements were made by weighing cut-outs of duplicate spectra. The capillary Me_4Si concentration was obtained by comparing the methyl resonance area of Me_4Si to the methyl resonance area of internal $(CH_3)_4NCl$ at known concentration. All high-field spectra were obtained at the probe temperature of 17°.

The concentration dependence of the histone IV high-field region PMR spectrum was obtained by diluting a histone IV solution (50 mg/ml) stepwise with pure D_2O or with 0.01, 0.05, 0.1, or 0.2 *M* NaCl in D_2O. In the salt concentration dependence studies, a given volume of 5 mg/ml of histone IV in D_2O (0.4 ml) was pipetted into a precision 5-mm NMR tube along with a few microliters of a concentrated salt solution (NaCl) and thoroughly mixed prior to spectral observation. The progressive dilution of the histone IV by addition of salt solution in these experiments was compensated by appropriate corrections in the salt concentration.

In the pD study, Bio-Rad Laboratories DCl or NaOD was added to ca. 0.6 ml of histone IV solution (ca. 4 mg/ml). Because only small amounts of NaOD or DCl were added during titration, the resultant concentration was not corrected. The error due to this factor was estimated to be less than 10%. The pD of each solution was measured in a small beaker with a Leeds and Northrup 7401 pH meter, equipped with miniature electrodes, and was taken to be the observed pH meter reading plus 0.4, the standard correction (Lumry et al., 1951). In each case the pD of the solution was measured before and after its PMR spectrum was taken. The differences were within ±0.1 pH unit.

Velocity sedimentation studies of histone IV in distilled water were performed with a Hermes Model E analytical ultracentrifuge. Absorption scans of 12-mm optical path

[1] Abbreviations used are: DPPH, 2,2-diphenyl-1-picrylhydrazyl; DSS, 2,2-dimethyl-2-silapentane-5-sulfonate.

Table I: Effect of Histone Concentration, $[H_0]$, on the PMR "Visibility," $([H_{obsd}]/[H_0]) \times 100\%$, of Histone IV High-Field Region PMR Bands.

PMR Band	Histone Concn, $[H_0]$ (M)			
	2.9	10	20	41×10^{-4}
I–VIII	63	57	35	27
I	61	45	29	21
II–V	67	59	40	32
VI	76	48	35	19
VII	41	32	24	23
VIII	66	54	33	29

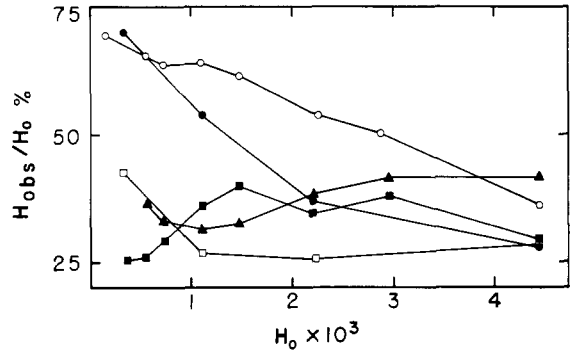

FIGURE 2: Effect of histone concentration on the pmr "visibility" of peak I protons. 0.0 (●); 0.01 (○); 0.05 (▲); 0.1 (■); 0.2 (□) M NaCl.

double sector cells were taken at 268 nm every 8 min and at 12000, 28000, and 44000 rpm. In these experiments, the temperature was maintained at 20° and distilled water was used as the reference solution.

Results

PMR Spectra. The 100-MHz (Boublik et al., 1970) and 220-MHz (Bradbury and Rattle, 1972) PMR spectra have previously been published for histone IV. Visual comparisons between the 220-MHz histone IV PMR spectra obtained here and those previously reported by Bradbury and Rattle (1972) indicate substantial agreements between the two groups of workers.

The 220-MHz PMR spectrum of histone IV in the high-field region is shown in Figure 1. The populations and chemical shifts of the protons from the various amino acid residues in histone IV are indicated by the height and position of the vertical lines shown at the bottom of Figure 1. These chemical shifts are based on corresponding shifts in random-coil proteins (McDonald and Phillips, 1969). Using these chemical shifts, the half-widths of their resonances in random-coil proteins (McDonald and Phillips, 1969) and the histone IV amino acid composition (DeLange et al., 1969; Ogawa et al., 1969), we have simulated the spectrum of monomeric, random-coil histone IV on the computer and these results are included in Figure 1 for comparison. The contribution of one methylated lysine out of 102 residues in histone IV is not included in the calculation as the chemical shifts of the protons in the corresponding amino acid are not available. No attempt was made to vary the individual PMR line positions and line widths in order to improve the correspondence between the calculated and experimental PMR spectra. Efforts to computer simulate the effects which segmental immobilization may have on the 220-MHz PMR spectrum of histone IV have previously been outlined by Bradbury and Rattle (1972).

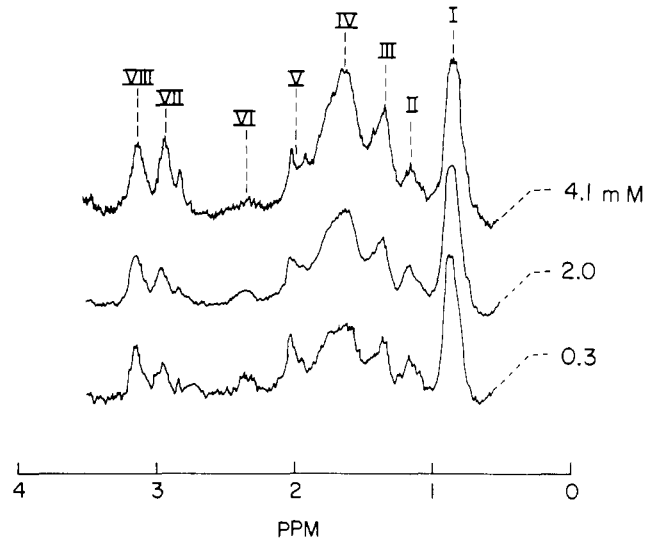

FIGURE 3: Effect of histone concentration on the 220-MHz PMR spectrum of histone IV in the high-field region. Protein concentration in mM, pD 3.7.

Table II: Effect of NaCl Concentration on the Percentage of "Visible" Histone IV Protons, $([H_{obsd}]/[H_0]) \times 100\%$, within Each High-Field Region PMR Band[a]

PMR Band	NaCl (M)				
	0	0.1	0.2	0.4	0.8
I	62	43	23	20	15
II	80	56			
III	82	70	61	61	61
IV	67	55	37	36	31
V	68	48	38	34	
VI	75				
VII	57	46	31	30	
VIII	77	59	32	21	

[a] $[H_0] = 4.2 \times 10^{-4}$ M histone IV.

Concentration Effects. Histone IV concentrations derived from averaged area measurements of the PMR bands consistently fall short of the total histone concentration, $[H_0]$ (Table I). As shown in Figure 2, the ratio, $[H_{obsd}]/[H_0]$, moreover, increases approximately threefold as the histone concentration is decreased from about 4×10^{-3} to 10^{-4} M at ionic strengths $\leq \sim 0.01$. At higher ionic strengths, however, $[H_{obsd}]/[H_0]$ appears, on the average, to remain relatively constant with stepwise dilution of histone IV. Among the individual PMR bands, peak VI reveals the greatest relative area deficit (Table I and Figure 3) but peak I (CH_3: Leu, Ile, Val) also displays a substantial area deficiency at the higher histone concentrations in pure D_2O. No significant frequency shifts were encountered upon varying the histone IV concentration.

Salt Effects. Table II shows the effects of NaCl on the PMR spectrum of histone IV. No significant chemical shifts were observed with the addition of NaCl. The relative extent of area loss among the various resonance peaks produced by NaCl at constant histone concentration is similar to that resulting from increasing the histone IV concentration at low ionic strengths.

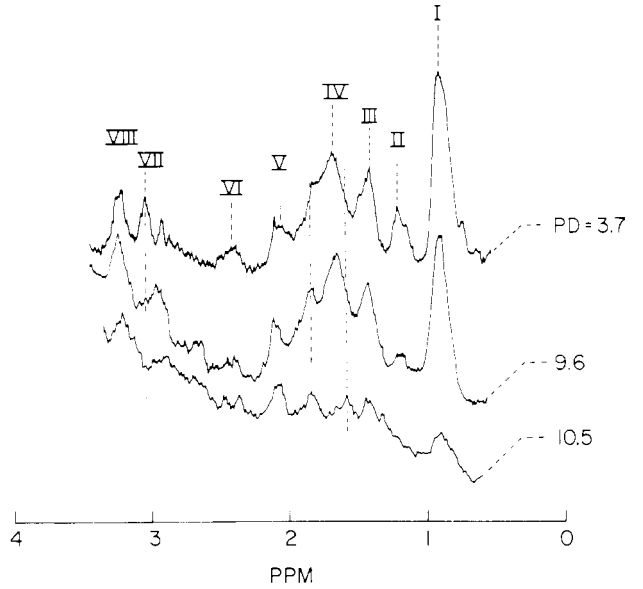

FIGURE 4: Effect of pD on the 220-MHz PMR spectrum of histone IV in the high-field region.

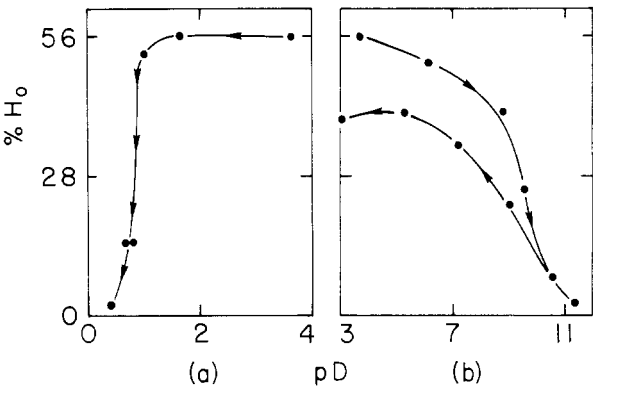

FIGURE 5: Observed variation in the intensty of peak I as a function of pD. The arrows shown indicate the direction of titration. $[H_0] = 3.34 \times 10^{-4}$ *M*.

pD Effects. Figure 4 shows the spectral changes in the PMR spectrum of histone IV as the pD is increased. In addition to resonance peak area losses (and histone IV precipitation) at the higher pD, as manifested for peak I in Figure 5b, peak VII is shifted upfield and peak IV is split into two subpeaks.

No significant peak area changes were observed when the pD was decreased from 3.7 to 1.0. However, as illustrated in Figure 5a, a sharp decrease in resonance area was observed at pD <0.8. Note that the solution remained perfectly transparent under these conditions. The spectrum of the histone IV at this low pD is similar to those obtained at higher histone IV or at higher salt concentrations. Peaks I, II, and VIII seem to exhibit greater area loss than peaks III, IV, and VII.

Discussion

Comparison of Calculated and Experimental PMR Spectra. Direct comparison of the calculated and observed (1.0×10^{-3} *M*) high-field PMR spectrum of histone IV (Figure 1) demonstrates that, except for peaks IV, V, and VI (see below), the measured band widths match those of a spectrum calculated from published random-coil data (McDonald and Phillips, 1969). Peak VI (Glu γ-CH_2) is 0.145 ppm downfield shifted from its counterpart in the calculated spectrum and its width is somewhat concentration dependent. The area of peak V is larger than expected, due, possibly, to a corresponding downfield shift of the Glu β-CH_2 protons and the resultant overlap with other resonances contributing to peak V.

Histone IV Aggregation. If we measure the PMR band areas in Figure 1, and compare each with its expected area based on the stoichiometric histone IV concentration, we find, in general, an area deficit. In Table I, for example, 43% of the protons, on the average, are missing from the PMR spectrum for a 1.0×10^{-3} *M* histone IV solution in pure D_2O, and 73% of the protons do not show up at a histone IV concentration of 4.1×10^{-3} *M*. We have attributed these area losses to the formation of molecular aggregates which give extremely broad PMR spectra. If this interpretation is correct, the corresponding equilibria between the predominantly random coil monomer and the PMR "invisible" histone IV complexes must entail a slow dissociation of the aggregates on the NMR time scale since there was no evidence for chemical exchange broadening of the monomer histone IV PMR spectrum, with the possible exception of peak VI (see Figure 3). In fact, for ionic strengths ≥0.05 (Figure 2) the ratio $[H_{obsd}]/[H_0]$ apparently does not vary significantly as $[H_0]$ is decreased upon dilution. In contrast, similar data for ionic strengths <0.05 indicate that this ratio increases significantly as $[H_0]$ is decreased. This difference in behavior may be related to the formation of large histone aggregates at ionic strengths >0.05 (Ui, 1957; Cruft et al., 1958; Edwards and Shooter, 1969; Diggle and Peacock,1971), which dissociate too slowly upon dilution to achieve equilibrium within the 1–2 hr between dilution steps. Since the apparent association constant, *K*, for histone aggregation at ionic strengths >0.05 is large (Cruft et al., 1958), we expect the aggregation *dissociation* rate constant, k_{-1}, to be much less than the *association* rate constant, k_1. If this is the case, the *initial* numbers of monomers and aggregates are merely diluted by the increased solution volume and the ratio $[H_{obsd}]/[H_0]$ should remain unchanged.

For the sake of discussion, let us assume that the measured areas are due to histone IV monomers in essentially the random-coil form. From the intensity measurements, it is then possible to ascertain the ratio of the histone IV random coil concentration ($[H_1]$) to the stoichiometric histone IV concentration $[H_0]$.

At low ionic strengths, a log–log plot of the monomer histone IV concentration, $[H_1]$, vs. the corresponding aggregate concentration, $[H_0] - [H_1]$, reveals a straight line correlation between these quantities (Figure 6).[2] This result suggests that an equilibrium between the random-coil monomer and the aggregates may involve only a single aggregate species at very low ionic strengths, *i.e.*

$$n\mathrm{H}_1 \rightleftharpoons \mathrm{H}_n \qquad (1)$$

[2] Only the peak I and averaged PMR data are represented here. The "error bars" extending from the averaged data denote the regions of the plot filled by PMR data from peaks I to VIII. These data are *not* distributed at random about the average data points. Rather they define a system of lines which are brought into coincidence by the least-squares analysis developed in the following paragraphs. The slopes and intercepts of these lines diverge only because the visibility, f_{1i}, of each PMR band "*i*," Table III, varies significantly from band to band.

For such an equilibrium

$$K = [H_n]/[H_1]^n \quad (2)$$

and since

$$[H_0] = [H_1] + n[H_n] \quad (3)$$

it is readily shown that

$$\log ([H_0] - [H]) = n \log [H_1] + \log (nK) \quad (4)$$

which predicts the linear log-log dependence mentioned above. The slope of this line is an estimate of the degree of aggregation, n, for the assumed aggregate species H_n and its intercept provides an estimate of the association constant, K. From least-squares analysis of the data, we obtained $n = 2.0$ and $K \approx 1000\ M^{-1}$.

The premise that only the random or extended coil form of monomeric histone IV contributes to the observed PMR spectrum has been tested by assuming, in the least-squares analysis, a simple dimerization model for histone IV aggregation in pure D_2O and including a fractional histone IV dimer contribution, f_2, to the histone IV PMR resonance areas. The best least-squares fit was obtained with $f_2 = 0.0$ for both peak I and the combined peak area data for the high-field region.

Since linear log-log plots are often misleading, we have attempted to analyze the data in another way. Let us assume that larger aggregates do exist in equilibrium with the histone IV monomers in pure D_2O, particularly at the higher histone IV concentrations. If these higher aggregates are formed by monomer association in a series of steps, this process can be described in terms of the following multiple equilibria:

$$\begin{aligned} H_1 + H_1 &\overset{K_2}{\rightleftharpoons} H_2 \\ H_1 + H_2 &\overset{K_3}{\rightleftharpoons} H_3 \\ &\text{----------} \\ H_1 + H_{n-1} &\overset{K_n}{\rightleftharpoons} H_n \end{aligned} \quad (5)$$

where H_1, H_2, ..., H_n denote the histone IV monomer, dimer, and n-mer, respectively, and K_2, K_3, ..., K_n are the corresponding association constants. Without real loss of generality, we can invoke the simplifying assumption:

$$K_2 \neq K_3 = K_4 = \ldots = K_n = K \quad (6)$$

where the supposition $K_2 \neq K$ is based on the above preliminary evidence for extensive dimer formation in pure D_2O. Since the stoichiometric histone concentration, $[H_0]$, may be written as

$$[H_0] = [H_1] + 2[H_2] + 3[H_3] + \ldots + n[H_n] \quad (7)$$

$$= [H_1] + K_2[H_1]^2 \sum_{n=2}^{\infty} n(K[H_1])^{n-2} \quad (8)$$

$$= [H_1] + K_2[H_1]^2 \frac{2 - K[H_1]}{(1 - K[H_1])^2} \quad (9)$$

it is readily shown that

$$\frac{1}{x^2} - \frac{1}{x} = 2K_2[H_0] \frac{1 - \frac{K}{2}[H_0]x}{(1 - K[H_0]x)^2} \cong 2K_2[H_0] \left\{1 + \frac{3}{2}K[H_0]x + \ldots\right\} \quad (10)$$

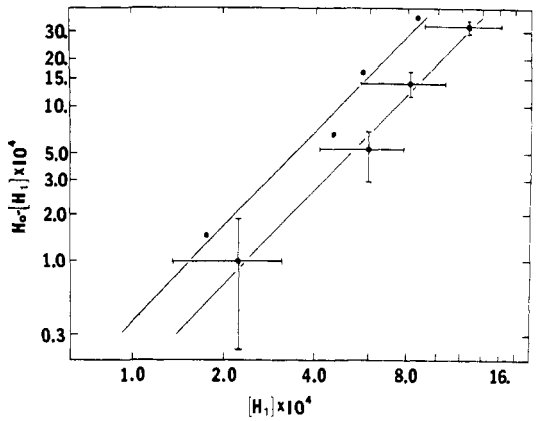

FIGURE 6: Log ($[H_0] - [H_1]$) vs. log $[H_1]$. Points without error bars were derived from the peak I data of Table I while the points with error bars have been obtained from the combined peaks I-VIII data of Table I.

The quantity $x = [H_1]/[H_0]$ can be determined from the observed resonance areas if we can assume that only monomeric histone IV contributes to the PMR spectrum. As expected, this analysis predicts a linear variation of the quantity $[(1/x^2) - (1/x)]$ vs. $[H_0]$ with slope equal to $2K_2$ in the limit of sufficiently low histone concentrations and for K sufficiently small such that $K[H_1] \ll 1$. However, at high histone concentrations, where formation of higher aggregates may become important, deviation from linearity would be expected, should it occur. We have found that the data for histone IV in pure D_2O (Table I) when plotted in this manner do not deviate significantly from that expected for simple dimer formation. Further analysis based on a least-square analysis of the data listed in Table I to eq 10 has permitted us to set an upper limit of $\sim 200\ M^{-1}$ to K, the stepwise association constant for the formation of the larger aggregates in pure D_2O. This result is consistent with the sedimentation studies of Cruft et al. (1958).

The foregoing analysis of the combined PMR data of Table I suggests that histone IV does not self-associate beyond the dimer stage in low ionic strength solutions. An important assumption in this analysis is that the histone IV monomer is entirely PMR "visible" and the dimer totally "invisible." Although the latter half of this assumption is not unreasonable for a compact rod-shaped dimer[3] of molecular weight 24,000 in the absence of significant segmental flexibility, the first half concerning the complete PMR "visibility" of the histone IV monomer warrants further scrutiny. The validity of this part of the assumption may be ascertained by similar log-log treatment of the data derived from the intensities of the individual PMR bands. Such treatment of the data for bands I, II-V, VI, VII, and VIII revealed similar linear log-log plots as for the combined data, except that the slopes of these lines often deviate from the expected slope of 2.0. These discrepancies may partly be due to the large experimental uncertainties associated with intensity measurements of the individual PMR bands. However, another factor may be that a portion of the histone IV monomer is also PMR "invisible." The observation that ~25% of the PMR intensity remains unaccounted for,

[3] The shape of the complex is being emphasized here, as it can have a profound influence on the PMR visibility. A protein molecule having an extended structure, e.g., β sheet, is expected to exhibit much broader PMR lines as compared with a globular protein of the same molecular weight due to the high anisotropy in its tumbling motion.

Table III: The Effect of Immobilizing Successive 10 Amino Acid Residue Segments of the Histone IV Sequence, Beginning with the C-Terminus, on the PMR "Visibility" of Individual PMR Bands.

PMR Band	Number of Mobilized Residues: 102	90	80	70	60	50	f_i Observed
	f_i Predicted						
I–VIII	1.00	0.87	0.81	0.71	0.57	0.50	0.76
I	1.00	0.96	0.78	0.78	0.61	0.48	0.60
II–V	1.00	0.89	0.82	0.68	0.62	0.53	0.88
VI	1.00	0.91	0.76	0.67	0.48	0.19	0.59
VII	1.00	0.83	0.78	0.61	0.50	0.39	0.62
VIII	1.00	0.88	0.88	0.77	0.71	0.65	0.79

even at histone concentrations approaching infinite dilution, provides plausibility for this hypothesis. Hence, the above treatment must be modified. If f_{1i} refers to the fraction of those protons contributing to an individual PMR band "i" which are PMR "visible," the apparent monomer histone concentration $[H_{obsd}]$, as calculated from the intensities of this band (Table I) will then be related to the true histone IV monomer concentration, $[H_1]$, by

$$[H_{obsd}] = [H_1] f_{1i} \tag{11}$$

An analogous expression may be written for the apparent histone IV monomer concentration derived from the combined intensity data. We write

$$[H_{obsd}] = [H_1] f_1 \tag{12}$$

f_1, the fraction of all the protons in the histone molecule which are contributing to the spectrum, can be shown to be an average of the f_{1i} weighted in accordance with the number of protons η_i contributing to each PMR band "i," i.e.

$$f_1 = \frac{\sum_i \eta_i f_{1i}}{\sum_i \eta_i} \tag{13}$$

Combining eq 12 with eq 2 and 3, we obtain the following modified equation to account for the PMR intensity variation observed with increasing histone concentration

$$K = \frac{f_1^{n-1}(f_1[H_0] - [H_{obsd}])}{n[H_{obsd}]^n} \tag{14}$$

f_1 and K can be extracted by least-squares analysis of the combined histone IV PMR data summarized in Table I. Assuming the occurrence of only dimer formation, i.e., taking $n = 2$, we obtained $K = 600\ M^{-1}$ and $f_1 = 0.76$. Using this value of K and the apparent monomer histone concentration $[H_{obsd}]$ derived from the areas of the individual PMR bands, we obtained the f_{1i} values listed in Table III. We note parenthetically that if 0.70 is taken as the *lower limit* for the histone IV monomer visibility, then it can be shown that 2 is the *maximum* integral value for n in eq 12 which will provide a reasonable least-squares fit to the peak I–VIII data of Table I.

Thus the study not only indicates that histone IV dimerizes in aqueous solutions of low ionic strength, but also suggests that this molecule possesses some stable, essentially PMR "invisible" secondary structure in its uncoiled state. This latter result is perhaps not surprising since PMR and CD studies of histone IV fragments obtained by CNBr cleavage (Pekary and Chan, 1975) indicate that the C-terminal portion of the polypeptide including about 20% of the histone IV sequence may be regarded as structured. In this connection we note that because of the high content of hydrophobic residues in the C-terminus (DeLange et al., 1969; Ogawa et al., 1969), this region of the histone IV molecule is the most likely to possess stable secondary structure. In fact, the "observed" f_{1i} values for the individual PMR bands of histone IV can be qualitatively accounted for by immobilization of the last 20–30 amino acid residues of the C-terminus. In Table III we summarize the effects of immobilizing successive 10 amino acid residue segments of the histone IV sequence beginning with the C-terminus. For a given structural immobilization, f_{1i} values have been computed for the various PMR bands by dividing the number of PMR visible protons contributing to the band by the total number of protons which will otherwise contribute to this band in the absence of motional restriction. A comparison of the f_{1i}'s so determined with the observed values led to an estimate of the aforementioned "break-point" between the hypothetical "structured" C-terminus and the "unstructured" N-terminus. Although this model only accounts for the observed pattern in the f_{1i}'s qualitatively, the agreement is reasonable considering the experimental uncertainties in the area measurements and that we have precluded the existence of other secondary structure in the remaining parts of the histone IV sequence.

Finally, although we have shown that histone IV dimerizes in aqueous solutions of low ionic strengths with an association constant of approximately 500–1000 M^{-1}, there is no evidence for the formation of higher aggregates under these conditions, a result which is corroborated by sedimentation velocity measurements. The value of $s_{20,w}$ measured for a 2.2×10^{-4} M histone IV solution was found to be less than 0.1 S at pH 3.3 in distilled water. Since the sedimentation velocity will be retarded by a factor of $1/(1 + n)$, n being the number of counterions bound (Bowen, 1970), the corrected sedimentation coefficient becomes less than 3 S if corrections are made for this primary charge effect. The PMR line widths of the resonances for these histone IV dimers are presumably too broad for the detection of these species, a result which implies that segmental motions in the polypeptides have become very slow and restricted on aggregation. Apparently the histone IV dimers are formed without extended free ends or loops.

Salt Effects. The α-helix content of histone IV is known to increase to a limiting value of about 20% at 0.1 M NaCl, beyond which no significant further increases are observed for NaCl concentrations up to 1.0 M (Bradbury et al., 1965; Jirgensons and Hnilica, 1965). On the other hand, we have observed area deficiencies in all the major PMR bands of histone IV even at low histone concentrations and in zero ionic strength, and these area losses increase uniformly with the NaCl concentration[4] (Table II). No conspicuous broadening of the resonances was noted when compared to the calculated spectrum of the random coil (except for peak VI)

[4] In these experiments, the rate at which equilibrium is attained after each increment in ionic strength will depend on the fast association rate constant, k_1, rather than the slow dissociation rate constant, k_{-1}, so troublesome for our dilution studies at intermediate ionic strengths. A thorough study of the time course of "β" histone aggregation as a function of ionic strength, histone concentration, pH, and temperature by Cruft et al. (1958) may be relevant to this problem. According to this study, "β-histone" (largely histone IV) reaches equilibrium within about 3 hr when the ionic strength of the solution is increased to 0.1 at 20°. Reattainment of equilibrium upon *dilution* under these conditions should then require days!

until the NaCl concentration of 0.8 *M* was reached. Since the observed pattern of area loss without broadening does not parallel the behavior expected for the salt-induced coil-to-helix transition of histone IV, the effects of NaCl on the PMR spectrum of this histone must be attributed almost entirely to the gross aggregation which predominates at ionic strengths greater than 0.1. This conclusion is corroborated by the earlier sedimentation results of Edwards and Shooter (1969), who reported sedimentation coefficients of 7 S to 20 S for histone IV aggregates in 0.1 *M* NaCl buffered at various pH values between 1 and 7. These sedimentation data, in fact, indicate that the number of histone IV molecules involved in an aggregate is probably very large.

Since PMR signals associated with aggregated histone IV molecules should escape detection in our experiments due to extreme broadening, the prominent *relative* area changes observed within the high-field region PMR spectrum with ionic strength increase (Table II) must be attributed to the formation of secondary structure within the histone IV *monomers*. PMR (Pekary et al., 1975) and circular dichroism studies (Pekary and Chan, 1975) on the cyanogen bromide fragments of histone IV support this view. The results obtained are consistent with the earlier conclusions of Bradbury and Rattle (1972) based on computer simulations of the histone IV spectrum.

pD Dependence. Figure 5 reveals substantial reduction in the PMR "visibility" of histone IV at high and low pD's. The area losses observed at high pD occur as the pD approaches the histone IV isoelectric point, p*I*, most certainly arise from increased aggregation and histone IV precipitation under these conditions (Cruft et al., 1958; Steinhardt and Beychok, 1964; DeLange et al., 1969). After precipitation at the higher pD, histone IV may be partially deaggregated by titrating back to neutral or acidic pD. As shown in Figure 5b, a hysteresis is observed. The ~30% additional area loss relative to the forward titration curve may be due to salt production and dilution of the sample during back titration.

The abrupt PMR area losses observed at pD <0.8 may be attributed to Cl^- anion condensation leading to increased histone IV aggregation (Davison and Shooter, 1956). As noted previously, the percentage of aggregated "β-histone" at 1.24% concentration, pH 5.4, rises from 38 to 87% within the ionic strength range 0.02–0.08 (Cruft et al., 1958). This ionic strength corresponds to the DCl concentration at which the observed precipitous drop in the histone IV PMR band areas occurs.

Significant upfield chemical shifts were observed for a number of resonances in the high-field region at high pD's. The upfield shift of peak VII (Lys ϵ-CH_2) is due to neutralization of the Lys-NH_3^+ group, p$K \simeq 10.4$ (Tanford, 1962). Such deprotonation also shifts the Lys δ-CH_2 + β-CH_2 resonances upfield so that the Arg β-CH_2 resonance becomes an isolated peak, as shown in Figure 4 for pD 9.6 and 10.5 (Arg-NH_2, p$K \simeq 12.0$) (Tanford, 1962).

Summary

PMR studies on histone IV have been carried out as a function of histone concentration, salt concentration, and pD. A significant proportion of the amino acid residues within the histone IV monomer was found to be PMR "invisible," even at histone IV concentrations approaching infinite dilution. This result suggested the existence of stable secondary structure within the hydrophobic C-terminal region. In the following paper, this superposition will be confirmed by the observation of a fully PMR "visible" histone IV fragment obtained by removal of just 18 residues from the C-terminus of the parent protein. Further loss of PMR resonance areas with increased histone IV concentration in pure D_2O, pD range 1–7, has been ascribed to the formation of histone IV dimers. Extensive histone IV aggregation occurred at pD <0.8 as well as in NaCl solutions of >0.01 ionic strength. Histone IV was found to precipitate from D_2O solutions at pD values near 11, the histone IV isoelectric point.

Acknowledgment

We thank Robert Watson for carrying out the histone IV velocity sedimentation experiments.

References

Boublik, M., Bradbury, E. M., and Crane-Robinson, C. (1970), *Eur. J. Biochem. 14,* 486.

Bowen, T. J. (1970), An Introduction to Ultracentrifugation, New York, N.Y., Wiley-Interscience.

Bradbury, E. M., Crane-Robinson, C., Goldman, H., Rattle, H. W. E., and Stephens, R. M. (1967), *J. Mol. Biol. 29,* 507.

Bradbury, E. M., Crane-Robinson, C., Phillips, D. M., Johns, E. W., and Murray, K. (1965), *Nature (London) 205,* 1315.

Bradbury, E. M., and Rattle, H. W. E. (1972), *Eur. J. Biochem. 27,* 270.

Cruft, H. J., Mauritzen, C. M., and Stedman, E. (1958), *Proc. R. Soc. London, Ser. B 149,* 21.

Davison, P. F., and Shooter, K. V. (1956), *Bull. Soc. Chim. Belg. 65,* 85.

Dearborn, D. G., and Wetlaufer, D. B. (1970), *Biochem. Biophys. Res. Commun. 39,* 314.

DeLange, R. J., Fambrough, D. M., Smith, E. L., and Bonner, J. (1969), *J. Biol. Chem. 244,* 5669.

Diggle, J. H., and Peacocke, A. R. (1971), *FEBS Lett. 18,* 138.

Edwards, P. A., and Shooter, K. V. (1969), *Biochem. J. 114,* 227.

Elgin, S. C. R., Froehner, S. C., Smart, J. E., and Bonner, J. (1971), *Adv. Cell Mol. Biol. 1, 1.*

Hoare, T. A., and Johns, E. W. (1971), *Biochim. Biophys. Acta 247,* 408.

Jirgensons, B., and Hnilica, L. S. (1965), *Biochim. Biophys. Acta 109,* 241.

Jirgensons, B., Hnilica, L. S., and Capetillo, S. C. (1966), *Makromol. Chem. 97,* 216.

Johns, E. W. (1964), *Biochem. J. 92,* 55.

Lewin, S. (1969), *J. Theor. Biol. 23,* 279.

Lewin, S. (1970), *Biochem. J. 119,* 62P.

Li, H. J., Isenberg, I., and Johnson, Jr., W. C. (1971), *Biochemistry 10,* 2587.

Li, H. J., Wickett, R., Craig, A. M., and Isenberg, I. (1972), *Biopolymers 11,* 375.

Lumry, R., Smith, E. L., and Glantz, R. R. (1951), *J. Am. Chem. Soc. 73,* 4335.

McDonald, C. C., and Phillips, W. D. (1969), *J. Am. Chem. Soc. 91,* 1513.

Ogawa, Y., Quagliarotti, G., Jordan, J., Taylor, C. W., Starbuch, W. C., and Busch, H. (1969), *J. Biol. Chem. 244,* 4387.

Pekary, A. E., Chan, S. I., Hsu, C.-J., and Wagner, T. E. (1975), *Biochemistry, 14,* following paper.

Pekary, A. E., and Chan, S. I. (1975), *Biochemistry*, (in press)
Shih, T., and Fasman, G. D. (1971), *Biochemistry 10*, 1675.
Smart, J. E., and Bonner, J. (1971), *J. Mol. Biol. 58*, 675.
Starbuch, W. C., Mauritzen, C. M., Taylor, C. W., Saroja, I. S., and Busch, H. (1968), *J. Biol. Chem. 243*, 2038.
Steinhardt, J., and Beychok, S. (1964), in The Proteins, Vol. II, 2nd ed, Neurath, H., Ed., New York, N.Y., Academic Press.
Tanford, C. (1961), Physical Chemistry of Macromolecules, New York, N.Y., Wiley.
Tanford, C. (1962), *Adv. Protein Chem. 17*, 69.
Tuan, D., and Bonner, J. (1969), *J. Mol. Biol. 45*, 59.
Ui, N. (1957), *Biochim. Biophys. Acta 25*, 493.
Wagner, T. E. (1970), *Nature (London) 227*, 65.

Nuclear Magnetic Resonance Studies on the Solution Conformation of Histone IV Fragments Obtained by Cyanogen Bromide Cleavage†

A. Eugene Pekary,‡ Sunney I. Chan,* Chen-Jung Hsu, and Thomas E. Wagner§

ABSTRACT: Two histone IV fragments obtained by cleavage at Met-84 by cyanogen bromide have been examined by proton magnetic resonance (PMR) spectroscopy as a function of temperature, peptide concentration, ionic strength, and pD. Sedimentation and gel electrophoresis studies on these peptides have also been carried out. The 220-MHz PMR spectrum of the N-peptide in both the high- and low-field regions was shown to be almost identical with that calculated for an extended coil N-peptide monomer. The calculated random coil and experimental C-peptide spectra, on the other hand, differ in many respects. Evidence was obtained for the presence of rigid secondary structure in the C-peptide. In addition, the Val, Leu, Ile CH_3 resonance displays a prominent high-field satellite band which shifts downfield with increasing temperature. Sedimentation studies on the N-peptide reveal the formation of extremely large, remarkably homogeneous aggregates at ionic strengths ≥0.01. The C-peptide, on the other hand, does not appear to form aggregates of sufficient size to be detectable in velocity sedimentation studies of a few hours duration. The relative area changes which have previously been noted in the PMR spectrum of histone IV with increasing ionic strength were also observed for the N-peptide but not the C-peptide. Interpretation of these relative area changes has been made in terms of the amino acid sequence of histone IV, and an effort was made to identify that segment of the polypeptide which undergoes secondary structural change with increasing ionic strength.

The histone IV amino acid sequence (DeLange et al., 1969; Ogawa et al., 1969) revealed a high proportion of basic residues within the N-terminal region and a preponderance of nonpolar side chains within the C-terminus. This unexpected amino acid distribution led to early suggestions (anonymous, 1968) that the conformation of this unusually structured protein, both as a free monomer and as a component of native chromatin, might provide important clues to its biological function.

A representative model (Sluyser, 1969) depicted histone IV as essentially a random coil monomer in solution and as a "hairpin" when complexed with DNA. The basic N-terminal region formed a strong electrostatic complex with DNA while the hydrophobic C-terminal region was either folded back along the N-terminal segment or weakly complexed with the same strand of DNA. This model remains attractive to many investigators (DeLange et al., 1972) because it leaves the C-terminal region relatively free to interact with other DNA molecules to form "cross-links" or with regulators of genetic replication and transcription.

The conformational significance of the clustering of the cationic residues of histone IV toward the N-terminal region is the subject of this as well as a previous communication (Pekary et al., 1975). The earlier paper was concerned with the conformational properties and the aggregation behavior of the intact histone IV molecule. In the present work, histone IV was cleaved at Met-84 by cyanogen bromide (CNBr) and the proton magnetic resonance (PMR) spectral characteristics as well as the sedimentation properties of the resultant N- and C-terminal fragments (hereafter referred to as the N- and C-peptides, respectively) have been examined under various conditions of peptide concentration, ionic strength, and pD. The conformational and aggregation properties of these peptides will be discussed in terms of their contributions to the structure and function of the parent histone IV protein molecule.

† From the Arthur Amos Noyes Laboratory of Chemical Physics, California Institute of Technology, Pasadena, California 91125 (Contribution No. 4924), and Cornell University Graduate School of Medical Sciences, New York, New York 10021. *Received July 18, 1974.* This work was supported by U.S. Public Health Service Grant GM-14523 from the National Institute of General Medical Sciences (to S.I.C.) and Grant CA-08748 from the National Cancer Institute (to T.E.W.).

‡ Population Council Postdoctoral Fellow, 1970–1972. Present address: Endocrinology Laboratory, Wadsworth VA Hospital, Wilshire and Sawtelle Boulevards, Los Angeles, California 90073.

§ Present address: Department of Chemistry, Ohio University, Athens, Ohio 45701.